JOURNAL OF MATERIALS SCIENCE **35** (2000) 699–705

Prediction of strength of recrystallized siliconcarbide from pore size measurement

Part I *The bimodality of the distribution*

N. ORLOVSKAJA
Institute for Problems of Materials Science, 3 Krzhizhanovskogo, 252 142 Kiev, Ukraine

H. PETERLIK, W. STEINKELLNER, K. KROMP
Institute of Materials Physics, University of Vienna, Boltzmanngasse 5, A -1090 Vienna, Austria
E-mail: Herwig.Peterlik@univie.ac.at

The bending strength values of more than 100 specimens of a recrystallized siliconcarbide ceramic (RSiC) show a distinct bimodal Weibull distribution. By measuring the number and size of surface pores, calculating the distribution of volume pores and choosing appropriate shape factors for the pores in the volume and for those close to the surface, the two modes of the Weibull distribution of the strength values can be predicted. © *2000 Kluwer Academic Publishers*

1. Introduction

To describe the fracture behaviour of brittle materials, the Weibull distribution has been widely used [1–3]. It is based on the "weakest-link hypothesis", which means that the most serious flaw controls the strength. If the number of the large pores, i.e. the ones, which are responsible for failure, is distributed according to an inverse power law, the strength values are distributed according to the Weibull distribution [2, 3]. Thus the statistical distribution of the flaw dimensions is closely connected to the fracture stresses obtained by mechanical tests. This relationship has been used to predict the distribution of flaw sizes and positions from different fracture experiments [4–8]. Reversely, a number of authors tried to predict fracture stresses from flaw populations [9–15], which would offer a non-destructive tool to measure mechanical properties. The application to ceramic materials faces two main problems [13]: Firstly, the defects in ceramics are usually small and secondly, the relation between the fracture strength and the size and geometry of the defect can be very complex. Thus, an experimental verification of the relation of the structure to the strength needs extensive fracture testing and a considerable fractographic effort. The difficulty is to obtain a reliable distribution in particular of the large pores. Scattering methods [16] or transmission electron microscopy give only information on the small pores [14], whereas mercury porosimetry [17] and impedance spectroscopy [18] cannot resolve the distribution with a sufficient precision. Though there are some new developments like magnetic resonance imaging [19, 20] or thermal nondestructive testing [21], the most widely used method to determine flaw distributions is digital image analysis in connection with scanning electron microscopy [22], X-ray imaging [23, 24], ultrasound microscopy [25–28] or optical methods (light microscopy [13, 24, 29] and transmission optical microscopy [14, 30]).

The reliability of the predictions of the mechanical properties from the measurement of pore size distributions is furthermore complicated, if a material does not perfectly obey the Weibull statistics. In particular, for ceramic fibres, this behaviour had been observed and attributed to the existence of different flaw populations, e.g. surface and volume flaws [31–33]. To improve the description of the experimental results, different ways were proposed, e.g. a modification of the two-parametric Weibull distribution [34], a bimodal lognormal distribution [35], generalized distributions assuming a Poisson flaw model without presuming a particular functional form [36], as well as bi- and multimodal Weibull distributions [32, 37, 38]. For ceramics, the bimodality due to different flaw populations has been more a theme of theoretical considerations than of experimental results [2, 3, 37]. The reason is probably the great experimental effort and the cost involved. The statistical scatter of the fracture strength of brittle materials requires a large number of specimens for statements based on reliable data. Therefore most papers dealt with the numerical simulation of experiments and investigated for example the precision of different evaluation procedures [39–43]. To cope with the statistical scatter, the strength values were determined by more than hundred tests and then compared to predictions made by non-destructive measurement of the pore size distribution determined by the measurement of an area of 16000 square millimeters. The large number of fracture strength data showed a distinct bimodality. The large area, from which the pore size distribution was measured, could be used to explain this bimodality by

being a consequence of the different shape factors of the pores in the volume and the pores close to the surface. The bimodality is important for practical reasons: if the size of the tested specimen does not coincide with the one of the future construction part, it is possible that the parameters of the "wrong" distribution are measured. For example, if the tested specimens are small, they could fail due to volume flaws, whereas large construction parts could fail due to surface flaws with much lower Weibull parameters. Thus, this work focuses in particular on the bimodality. The limitations by a distribution being not exactly power-law distributed or by a limited measured area (limited number of pores) are discussed separately [44].

2. Materials and methods

The material investigated was a recrystallized silicon-carbide. This material has a high strength in relation to its density and is nearly free of second phases (sintering aids) except for a rest of free silicon (<1 wt.%). Thus it is highly creep resistant. A high thermal conductivity and a low thermal coefficient of expansion allow this material to be applied for kiln furniture in the ceramic industry. A short description of the material may be found in [43, 45], a precise description of processing and texture in [46].

More than hundred specimens, which were tested in four-point bending in a previous work [43] were ground and polished to a final mesh of 1 μm. Each of these specimens was investigated in the optical microscope. Fig. 1 shows a micrograph of the material, which represents an area of 4.44 square millimeters. As it is clearly visible, the material is highly porous. From a technical point of view this has the advantage that the density is relatively low and thus the material contributes to energy saving when used as kiln furniture [47]. With respect to our investigation of the relationship between pore size distribution and strength, this high porosity has the advantage that the dimensions of a large number of pores could be collected easily. From each of the mechanically tested specimens 25 to 30 of such micrographs were taken and subsequently evaluated by digital image processing. The maximum and the minimum pore size, the maximum and minimum pore size in the specific directions of the long axis of the specimen and perpendicular to this axis as well as area and perimeter were measured.

3. Theoretical considerations

If linear elastic fracture mechanics (LEFM) is presumed and the frequency distribution of pore size $g(a)$ decreases with an inverse power law with an exponent r and a scaling pore size a_{sc}, the fracture probabilities P_f are Weibull distributed with an exponent m and a scaling parameter σ_0 [1–3]:

$$g(a) = g(a_{sc})\left(\frac{a}{a_{sc}}\right)^{-r} \rightarrow P_f = 1 - \exp\left(-\left(\frac{\sigma}{\sigma_0}\right)^m\right) \tag{1}$$

By this, the parameters of the pores $(g(a_0), r)$ and the ones of the strength (σ_0, m) are related by [2, 3]

$$m = 2(r-1) \qquad \text{and}$$
$$\sigma_0 = \left(\frac{m}{(2a_{sc}g(a_{sc})V_0)}\right)^{1/m} \frac{K_{Ic}}{\left(Y(\pi a_{sc})^{1/2}\right)}, \tag{2}$$

where V_0 is the effective tested volume, K_{Ic} the critical fracture toughness and Y the shape factor.

There are the following difficulties:

- Firstly, fracture toughness K_{Ic} has to be known. In this work it was measured by an independent

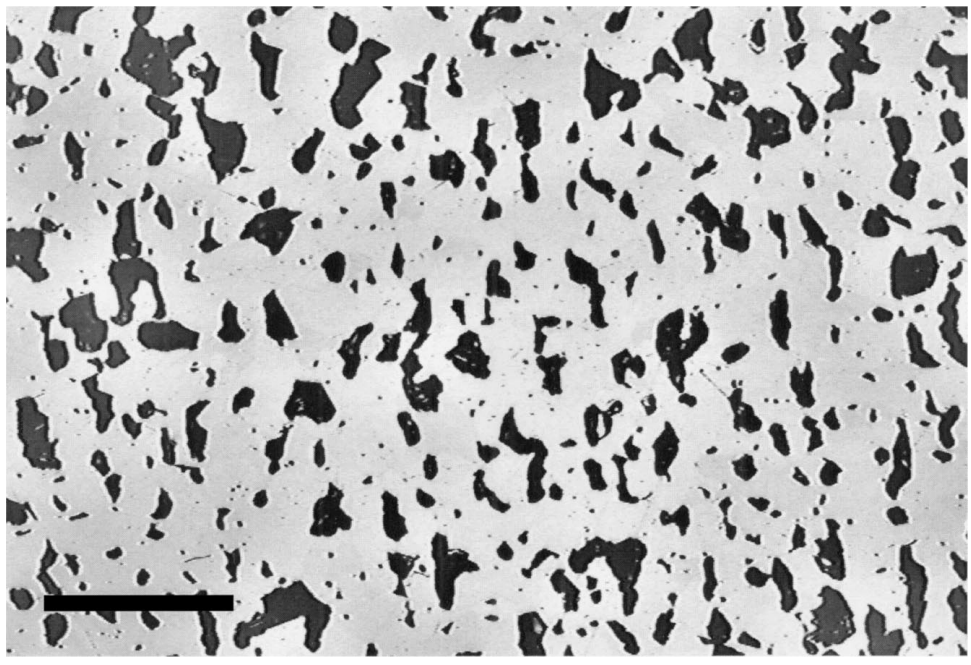

Figure 1 Micrograph of the porous RSiC. The bar equals 500 microns.

procedure (single edge notched beam, notched by a diamond blade with a thickness of 50 microns, resulting in a notch radius of about 30 microns). Five tests were performed according to the German prestandard DIN 51109. The fracture toughness turned out to be 2.05 ± 0.1 MPa $\sqrt{\text{m}}$. A comparison of this test method to others could be found in literature with data obtained by a round robin test for five different brittle materials [48].

- Secondly, the shape factor Y has to be determined.
- Thirdly, the volume frequency distribution of the pore sizes has to be known. In the following the way to calculate it from the measured surface distribution will be investigated. The consequences due to a limited number of pores (i.e. a limited area measured) and a distribution, which does not perfectly obey a power-law, were investigated separately [44].

To calculate the volume distribution from the surface distribution determined by the microscope, in a first approximation the shape of the pores is assumed to be spherical and the dependence of the number on the size should be distributed according to a power law, Equation 1. These assumptions allow an analytical expression to relate the number of pores in an unit volume to the one in an unit area instead of numerical procedures, e.g. the Schwartz-Saltykov diameter method [13] or the 3D-fibre orientation reconstruction from image analysis [49].

The probability to find a pore of a certain size, denoted by a, by a plane cut out of a certain volume is a/L (Fig. 2). Thus the total number of pores in a surface S, observed in an interval $[a, a + \mathrm{d}a]$, is related to the number of pores in a volume V by

$$N^{\text{tot},S}_{\text{in}[a+\mathrm{d}a]} S = N^{\text{tot},V}_{\text{in}[a+\mathrm{d}a]} V \frac{a}{L} = N^{\text{tot},V}_{\text{in}[a+\mathrm{d}a]} a S \qquad (3)$$

By integration over all possible pore sizes a the distributions of surface and volume pores, g_s and g_v, are related by

$$\int_0^\infty \mathrm{d}b\, g_\text{s}(b) = \int_0^\infty \mathrm{d}a\, a g_\text{v}(a) \qquad (4)$$

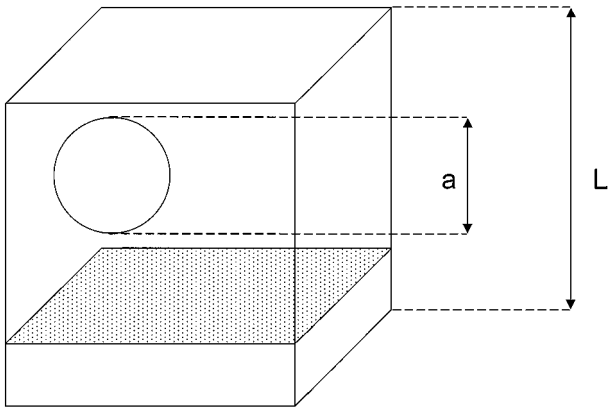

Figure 2 The probability to find a pore in a volume by an arbitrary plane cut is a/L.

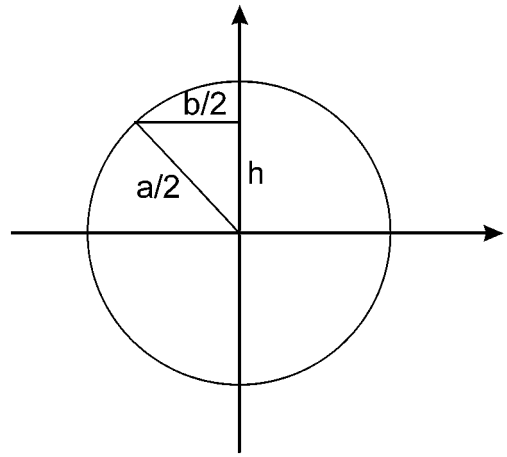

Figure 3 Dependence of a (diameter of spherical volume pores) to the observed length b (diameter of surface pores), if a plane cut is performed.

With the assumption that both, the surface and the volume pores, obey an inverse power law (Equation 1), and by use of the following identity (see Fig. 3),

$$b = 2\sqrt{(a/2)^2 - h^2} \qquad \text{and}$$
$$1 = \frac{2}{a}\int_0^{a/2} \mathrm{d}h = \int_0^a \mathrm{d}b \frac{b}{a\sqrt{a^2 - b^2}} \qquad (5)$$

the relation of the surface and the volume pores can be calculated:

$$\begin{aligned}\int_0^\infty \mathrm{d}b\, g_\text{s}(b) &= \int_0^\infty \mathrm{d}a\, a g_\text{v}(a) \\ &= \int_0^\infty \mathrm{d}a\, a g_\text{v}(a) \int_0^a \mathrm{d}b \frac{b}{a\sqrt{a^2 - b^2}} \\ &= \int_0^\infty \mathrm{d}a\, a g_\text{v}(a) \int_0^\infty \mathrm{d}b \frac{b\Theta(a-b)}{\sqrt{a^2 - b^2}}, \qquad (6)\end{aligned}$$

where Θ is the Heaviside step-function. Performing a change of the integrations and inserting the power law (Equation 1) into Equation 6 leads to

$$\int_0^\infty \mathrm{d}b\, g_\text{s}(b) = \int_0^\infty \mathrm{d}b \int_0^\infty \mathrm{d}a\, g_\text{v}(a) \frac{b}{\sqrt{a^2 - b^2}} \qquad (7)$$

With the substitution $b = ax$ the integration can be analytically performed, with the indices s and v denoting the parameters of the surface and volume distribution of pores, respectively:

$$\begin{aligned} r_\text{v} &= r_\text{s} + 1 \\ g_\text{v}(a_\text{sc}) &= \frac{g_\text{s}(a_\text{sc})}{(a_\text{sc} G)} \qquad \text{with} \\ G &= \sqrt{\frac{\pi}{2}} \frac{\Gamma(r_\text{s}/2 + 1/2)}{\Gamma(r_\text{s}/2 + 1)} \qquad (8)\end{aligned}$$

where Γ is the Gamma-function. From this equation and Equation 2 the parameters of the Weibull distributed strength values follow immediately. Because a spherical shape of the pores was assumed, this model

is a certain simplification. The calculated results, however, will confirm that despite these approximations reasonable predictions about the mechanical strength are obtained.

Now, if the pores are homogenously distributed, it is obvious that a part of the pores is located in the volume and a part close to the surface. They both are accompanied by different shape factors. It is thus convenient to describe the mechanical fracture behaviour by the existence of a single flaw population with two different shape factors, the one for the volume pores Y_v and the other for the surface pores Y_s. In a first approximation, the shape factor of an elliptical pore with axes a_0,b_0 in an infinite body in tension is given by [50]:

$$Y_v(\theta) = \frac{b_0}{a_0 E(k)} \left(\sin^2(\theta) + \left(\frac{a_0}{b_0}\right)^2 \cos^2(\theta) \right)^{0.25} \quad \text{with}$$

$$k = \sqrt{1 - \left(\frac{b_0}{a_0}\right)^2} \tag{9}$$

for $a_0 > b_0$, $E(k)$ being the complete elliptic integral of the second kind. The subscript zero characterizes the long axis of an elliptical pore, which is related to the pore diameter a measured by the microscope by $a_0 = a/2$. As the pores are arbitrarily oriented, numerical integration of the shape factor with respect to its angle and inserting the ratio maximal to minimal pore length, which was obtained by the pore size measurements as the mean of all measured pores, $b_0/a_0 = b/a = 0.63$, gives:

$$Y_v = \frac{2}{\pi} \int_0^{\pi/2} \mathrm{d}\theta \; Y_v(\theta) = 0.555 \tag{10}$$

The shape factor for the surface pores is given by the area of the crack on the plane of maximal stress [51], which is, for an elliptical crack, the area $= a_0\, b_0\, \pi$:

$$Y_s = 0.65 \sqrt{a_0^{-1} \sqrt{\text{area}}} = 0.771 \tag{11}$$

The amount of specimens fracturing from surface defects β could be estimated by the relative amount of critical surface pores. Each surface pore has an effective length a_{eff}, which is obtained by the mean of the length. This corrects that not each pore is touching the surface (if this is the case, the effective length would equal to $2\, a_0$), but may be partly cut by the surface:

$$a_{\text{eff}} = \frac{1}{a} \int_0^a \mathrm{d}x \; x = \frac{1}{2} a \tag{12}$$

Then the relative amount of surface pores, which are critical, is obtained similarly to Fig. 1 by the probability of a pore being located on the tensile surface, which is $P_s = a/W$ (W being the width of the specimen). Inserting the scale parameter for the surface pores and their shape factor, a mean critical length is estimated from Griffith theory:

$$a_c = \left(\frac{K_{Ic}}{\sigma_{0s} Y_s \sqrt{\pi}} \right)^2 \tag{13}$$

The amount of fractures from surface pores β is then calculated by the relative amount of critical surface pores from all critical pores (the factor two in the lower integration limit arises, because a_c is only the long axis of the ellipse, the total length of the pore being twice that value):

$$\beta = \frac{\int_{2a_c}^{\infty} \mathrm{d}a \; \frac{a_{\text{eff}}}{W} g(a)}{\int_{2a_c}^{\infty} \mathrm{d}a \; g(a)} = \frac{\int_{2a_c}^{\infty} \mathrm{d}a \; \frac{a}{2W} g(a)}{\int_{2a_c}^{\infty} \mathrm{d}a \; g(a)} \tag{14}$$

4. Results and discussion

If a specimen contains different flaw populations, they all contribute to the failure probability [2, 32, 37]:

$$P_f = 1 - \exp\left(-\left(\frac{\sigma}{\sigma_{01}}\right)^{m_1} - \left(\frac{\sigma}{\sigma_{02}}\right)^{m_2} \right) \tag{15}$$

This equation is valid, if the distributions are independent, continuous and both equally frequent and present in all specimens. In the case of a sufficiently small test volume this is not generally valid: If for example one distribution has a low scale parameter, but the number of the defects is small, only a small number of specimens will fail due to this distribution. One possibility is to correct Equation 15 by a parameter, which describes

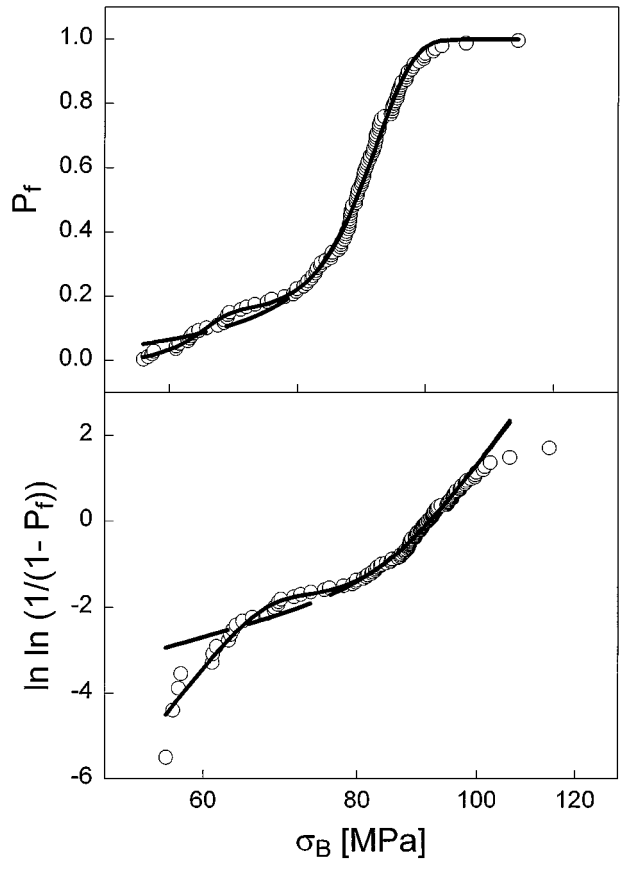

Figure 4 Fracture strength values (circles). Solid line: Fit by the additive bimodal Weibull distribution (Equation 16), dashed line: fit by the multiplicative bimodal model (Equation 15). For low strength values, the fit results differ, for high values they coincide.

the relative number of defects of both distributions, the other is to use an additive Weibull equation [38]:

$$P_f = \left[1-(1-\alpha)\exp\left(-\left(\frac{\sigma}{\sigma_{01}}\right)^{m_1}\right) + \alpha\exp\left(-\left(\frac{\sigma}{\sigma_{02}}\right)^{m_2}\right)\right] \quad (16)$$

Two parameters describe each of the respective Weibull distributions, σ_{01}, m_1, σ_{02}, m_2, and one parameter α the effectiveness of each distribution, i.e. which of the distributions was responsible for failure. Because the surface pores have a higher shape factor, they fracture first (compare Equations 10 and 11). The relative amount of critical surface to volume pores is described by the parameter β. Thus, if the last term in Equation 16 denotes the surface distribution, α from the mechanical tests is equal to β from the pore size measurements, i.e. $\alpha = \beta$.

Fig. 4 shows the typical Weibull plot for the measured strength values, the upper diagram with a linear and the lower with a logarithmic scale. A distinct bimodality of the fracture strength could be observed from this diagram. The circles represent the measured

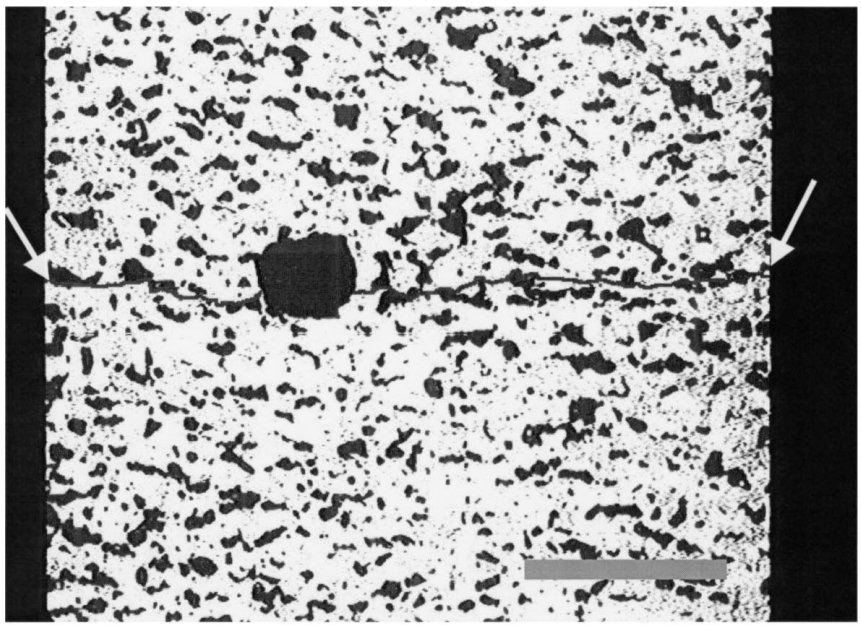

(a)

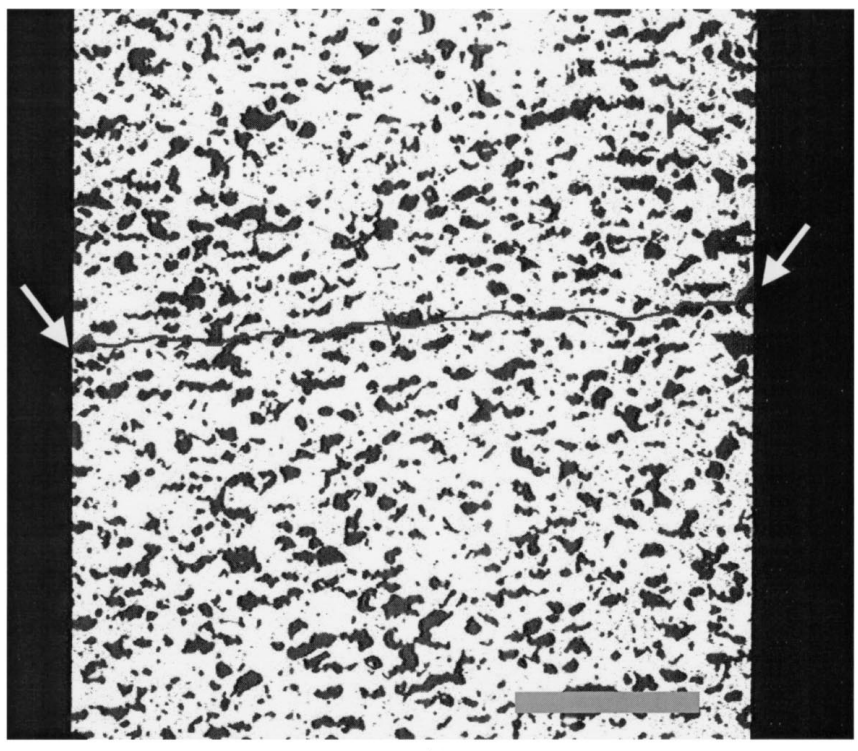

(b)

Figure 5 Specimen surfaces with fracture lines after test (between arrows). The bar equals 1 mm. a) huge surface pore could be identified as fracture origin (upper picture), b) surface and volume pores could not be distinguished as fracture origin (lower picture).

strength values, the dashed line a fit by Equation 15 (multiplicative bimodal Weibull distribution), the solid line by Equation 16 (additive bimodal Weibull distribution). For low strength values, the fit results differ, for high strength values, they coincide. But it can clearly be seen that the additive equation better describes the experimental results.

The results from the mechanical tests are now compared to those obtained from measurements of the distribution of pore sizes. This is performed under the assumption that the pore dimension perfectly obeys the power law (Equation 1). From the measurement of 16000 square millimeters of polished surface of RSiC, the fit parameters obtained for a scaling pore size $a_{sc} = 200$ microns were

$$g_s(a_{sc}) = 4.312 \times 10^8\,\mathrm{m}^{-3} \text{ and } r_s = 6.694. \quad (17)$$

Note that g_s is the frequency distribution density of surface cracks (dimension m^{-3}) and not the defect density, which is obtained by integration over the crack length. The values for the surface parameters are inserted into Equation 8 to calculate the volume parameters:

$$g_v(a_{sc}) = 4.935 \times 10^{12}\,\mathrm{m}^{-4} \text{ and } r_v = 7.694, \quad (18)$$

from which $m_v = 2(r_v - 1) = 13.4$ can be computed. With the knowledge of the fracture toughness, 2.05 ± 0.1 MPa $\mathrm{m}^{1/2}$, the strength immediately follows from Equation 2.

The strength values from an unimodal Weibull fit are shown in the first column of Table I, the ones from a bimodal fit in the second and the values calculated from the pore size measurement in the third column of Table I. The predicted scale parameters correspond perfectly to the ones obtained from the mechanical tests. The Weibull modulus from the pore size measurement is 13.4, whereas the bimodal fit from mechanical tests results in 16.1. Monte-Carlo simulations have shown that the variation coefficient of the modulus is generally about ten times the one of the scale parameter [42]. For a material perfectly obeying the Weibull distribution the variation coefficient from 123 mechanical tests $\Delta m/m$ is nearly 8% [42] and it could be even much larger for a bimodal material [43]. This should explain qualitatively the observed higher deviation for the predicted values for the Weibull modulus. Additionally, the relative amount of fractures due to surface pores, the parameter α, was obtained by inserting a critical length of $a_c = 484$ microns obtained from Equation 13 as lower integration limit into Equation 14 and is close to the same parameter obtained by the fit from the mechanical tests.

TABLE I Comparison of bimodal Weibull parameters from the fit of the strength values and the calculation from pore size distribution

Parameters	Unimodal Weibull-fit	Bimodal Weibull-fit	Calculation from pore size
σ_{01}	93.6 MPa	92.5 MPa	94.7 MPa
$m_1 = m_2$	9.8	16.1	13.4
σ_{02}		64.8 MPa	68.2 MPa
α		13.7%	14.7%

Unfortunately, it is not possible to determine the relative amount of fractures from surface pores α by fractography. Fig. 5a,b show binary pictures of two specimen surfaces before the fracture test, and an additional gray line depicts, where fracture occurred. Only in some rare cases (Fig. 5a) a huge pore can be identified as the fracture origin, but usually one cannot distinguish between surface or volume fractures (Fig. 5b). Even in a subsequent fracture analysis the rough surface (due to the high porosity) and the lack in fracture mirrors and fracture lines prevents from an unique identification of fracture origins.

5. Conclusion

The aim of this work was to show that with very simple assumptions a reasonable value for the strength distribution of a porous ceramic material can be obtained. Due to this simplifications there exist a lot of possibilities to improve the reliability of the predicted strength values. The first improvement could be to calculate precise shape factors, if the geometry is well known. A second improvement is to take into account the interaction of pores and the shielding of the stress field by neighbouring flaws. Another possibility could be the direct determination of the three-dimensional pore distribution by appropriate censoring techniques, e.g. x-ray imaging or acoustical microscopy. This would make obsolete the simplifying assumption of a sherical shape of the pores. It was, however, not the goal to find a perfect solution, which completely describes the fracture behaviour, but to show that with some simple estimations a reasonable result for the fracture strengths could be obtained from pore size measurements and that moreover the bimodality of the Weibull distribution found a simple explanation.

Of course, the experimental verification was performed for recrystallized siliconcarbide as a model material. Due to the high porosity of this material and the good contrast between pores and material it is relatively easy to assemble a sufficiently large number of pore size data. It should be noted that the required effort could increase considerably for other ceramics. However, the method seems to be of great practical interest, as it offers the possibility to predict the mechanical behaviour from non-destructive pore size measurements during industrial processing. The development of future new automatic techniques to measure small structures in three dimensions will offer additional possibilities to enhance the prediction of the mechanical properties of materials by non- destructive testing.

Acknowledgements

The authors thank for the financial support by the Austrian Ministery of Science under project nr. GZ 45.389/2-IV/3a 95 in the frame of the European COST 510 joint project D37-D19-D45-A9, and by the Austrian exchange program for Middle- and Eastern Europe. We thank Mr. W. Heider, Cesiwid Erlangen

(now: Shanghai TOKAN Ceramics) for supplying the material.

References

1. W. WEIBULL, *J. Appl. Mech.* **18** (1951) 293.
2. R. DANZER, *J. Europ. Ceram. Soc.* **10** (1992) 461.
3. L. SIGL, *Z. Metallkd.* **83** (1992) 518.
4. A. S. ARGON, *Proc. Roy. Soc.* **A250** (1959) 422.
5. J. D. POLONIECKI and T. R. WILSHAW, *Nature* **229** (1971) 226.
6. J. R. MATTHEWS, F. A. MCLINTOCK and W. J. SHACK, *J. Amer. Ceram. Soc.* **59** (1976) 304.
7. A. G. EVANS and R. I. JONES, *ibid.* **61** (1978) 156.
8. P. D. WARREN, *J. Europ. Ceram. Soc.* **15** (1995) 385.
9. J. LAMON, *J. Amer. Ceram. Soc.* **71** (1988) 106.
10. B. SCHULSTRICH and M. FÄHRMANN, *J.Mater. Sci. Lett.* **3** (1984) 597.
11. D. KOVAR and M. J. READY, *J. Amer. Ceram. Soc.* **79** (1996) 305.
12. T. HOSHIDE and M. MASUDA, *Mater. Sci. Res. Int.* **1** (1995) 108.
13. C.LUEN-YUAN and D. K. SHETTY, *J. Amer. Ceram. Soc.* **75** (1992) 2116.
14. Y. ZHANG, N. UCHIDA, K. UEMATSU, T. HOTTA, K. NAKAHIRA and M. NAITO, *Key Eng. Mat.* **159–160** (1999) 269.
15. J. LAMON, *Revue-de-Metallurgie*. **92** (1995) 265.
16. G. G. LONG and S. KRUEGER, *J. Appl. Cryst.* **22** (1989) 539.
17. J. LLAVSKY, C. C. BERND and J. KARTHIKEYAN, *J. Mater. Sci.* **32** (1997) 3925.
18. L. DESSEMOND and M. KLEITZ, *J. Europ. Ceram. Soc.* **9** (1992) 35.
19. P.J. PRADO, B. J. BALCOM, S. D. BEVEA, T. W. BREMNER, R. L. ARMSTRONG, R. PISHE and P. E. GRAFTEN-BELLEW, *J. of Physics D (Applied Physics)* **31** (1998) 2040.
20. J. H. STRANGE and J. B. W. WEBBER, *Meas. Sci. Techn.* **8** (1997) 555.
21. V. G. SEVAST'YANENKO, D. A. RUSAKEVICH, A. A. RUSAK and M. T. KOLESNIKOVA, *J. of Eng. Phys. and Thermophys.* **66** (1994) 380.
22. G. BONIFAZI and E. PROVERBIO, *Scanning Microscopy* **10** (1996) 59.
23. D. J. COTTER, W. D. KOENIGSBERG, R. E. WYSNEWSKI and G. HAMILTON, *J. Amer. Ceram. Soc.* **73** (1990) 1763.
24. U. MUCKE, T. RABE and J. GOEBBELS, *Praktische Metallographie* **35** (1998) 665.
25. A. BRIGGS, "Advances in Acoustic Microscopy," Vol. 1 (Plenum Press, New York, London, 1995).
26. A. BRIGGS and W. ARNOLD, "Advances in Acoustic Microscopy," Vol. 2 (Plenum Press, New York, London, 1996).
27. D. J. ROTH, D. B. STANG, S. M. SWICKARD, M. R. DEGUIRE and L. E. DOLHERT, *Materials Evaluation* **49** (1991) 883.
28. T. NONAKA, Y. HAYAKAWA, S. TAKEDA, H. NISHIMORI and S.YAMAGUCHI, *J. Europ. Ceram. Soc.* **6** (1990) 9.
29. N. UCHIDA and L. BERGSTROM, *ibid.* **17** (1997) 1193.
30. K. UEMATSU, Y. ZHANG, N. UCHIDA, T. HOTTA, M. NAITO, N. SHINOHARA and M. OKUMIYA, *Key Eng. Mat.* **161–163** (1999) 145.
31. E. BOURGAIN and J. J. MASSON, *Comp. Sci. Techn.* **43** (1992) 221.
32. K. GODA and H. FUKUNAGA, *J. Mater. Sci.* **21** (1986) 4475.
33. M. L. GAMBONE, *Scripta Mat.* **34** (1996) 507.
34. K. K. PHANI, *J. Mater. Sci.* **23** (1988) 2424.
35. S. H. OWN, R. V. SUBRAMANIAN and S. C. SAUNDERS, *ibid.* **21** (1986) 3912.
36. S. DURHAM, J. D. LYNCH and W. J. PADGETT, *J. Compos. Mat.* **22** (1988) 1131.
37. D. SONDERMAN, K. JAKUS, J. E. RITTER JR., S. YUHASKI JR., and T. H. SERVICE, *J. Mater. Sci.* **20** (1985) 207.
38. T. JUNG, R. V. SUBRAMANIAN and V. S. MANORANJAN, *ibid.* **28** (1993) 4489.
39. J. RITTER, N. BANDYOPADHYAY and K. JAKUS, *Amer. Ceram. Soc. Bull.* **60** (1981) 798.
40. B. BERGMAN, *J. Mater. Sci. Lett.* **3** (1984) 689.
41. A. KHALILI and K. KROMP, *J. Mater. Sci.* **26** (1991) 6741.
42. H. PETERLIK, *ibid.* **30** (1995) 1972.
43. N. ORLOVSKAJA, H. PETERLIK, M. MARCZEWSKI and K. KROMP, *ibid.* **32** (1997) 1903.
44. H. PETERLIK, N. ORLOVSKAJA, W. STEINKELLNER and K. KROMP, *ibid.* **35** (2000) 707.
45. A. KHALILI, H. PETERLIK, J. DUSZA and K. KROMP, in Proc. of the Intern. Fractography Conf. (Oktober 1994) (Polygrafia SAV Bratislava, Stará Lesná, Slovakia, 1994) p. 72.
46. J. KRIEGESMANN, M. KRAUS and A. GROS, *CFI (Ceram.For.Int.)-Ber.DKG* **75** (1998) 83.
47. H. PETER, *Silicates Indust.* **46** (1981) 179.
48. R. J. PRIMAS and R. GSTREIN, *Fatigue and Fract. of Eng. Mat. Struct.* **20** (1997) 513.
49. Y. T. ZHU, W. R. BLUMENTHAL and T. C. LOWE, *J. Compos. Materials* **31** (1997) 1287.
50. Y. MURAKAMI, "Stress Intensity Factors Handbook," Vol. 2 (Pergamon Press, Oxford 1987) p. 684.
51. *Idem., ibid.* Vol. 2 (Pergamon Press, Oxford, 1987) p. 822.

Received 3 April 1998
and accepted 22 July 1999